Enhanced Least-Squares Positioning Algorithm for Indoor Positioning

Ian Sharp and Kegen Yu, *Senior Member*, *IEEE*

Abstract—This paper presents an enhanced least-squares positioning algorithm for locating and tracking within indoor environments where multipath and nonline-of-sight propagation conditions predominate. The ranging errors are modeled as a zero-mean random component plus a bias component that is assumed to be a linear function of the range. Through minimizing the mean-square error of the position estimation, an expression for the optimal estimate of the bias parameter is obtained. Both range and pseudo-range-based positioning are considered. Simulations and experimentation are conducted which show that a significant accuracy gain can be achieved for range-based positioning using the enhanced least-squares algorithm. It is also observed that the pseudo-range-based least-squares algorithm is little affected by the choice of the bias parameter. The results demonstrate that the experimental 5.8-GHz ISM band positioning system can achieve positional accuracy of around half a meter when using the proposed algorithm.

Index Terms—Indoor positioning, positional accuracy analysis, enhanced least-squares algorithm, multipath and nonline-of-sight propagation, range and pseudo-range, optimal bias parameter, experimental verification

1 Introduction

The development of radiolocation technology initially was associated with outdoor terrestrial systems such as LORAN [1], but more particularly in recent decades with the satellite-based global positioning system (GPS) [2], [3]. Such systems calculate positions either from the determination of range based on time-of-flight measurements or more commonly by the application of pseudo-ranges estimated from time-of-arrival (TOA) measurements. A pseudo-range is the euclidean range between a transmitter-receiver pair plus an unknown offset common to all the TOA measurements. Such outdoor systems typically have close to line-of-sight (LOS) conditions from the mobile unit to the "fixed" base stations (BSs) or satellites, so that ranging errors are typically assumed to be random with a zero mean. A review of the performance of range and pseudo-range positioning in relationship to the Cramer-Rao lower bound (CRLB) for the LOS case given in [4] shows that the range (TOA) positioning accuracy is generally better than the equivalent pseudo-range positioning using time difference of arrival (TDOA), but with geometric spatial symmetry relative to the location being determined the two estimates have equivalent accuracy. For this random-error only case, the iterative least-squares (LS) algorithm [5, Chapter 7] is a computationally simple yet effective method of determining position from either range or pseudo-range data. The LS approach is optimal in the presence of statistically independent zero-mean Gaussian range measurement errors with the same standard deviation (STD) in each receiver [6]. Although other errors do occur, in particular due to multipath propagation, the LS approach generally performs well in outdoor environments.

More recently, radiolocation technology has been extended to indoor environments for applications such as tracking people and assets [7], [8], [9], [10], [11]. In such indoor environments, GPS does not work well as the satellite signals are blocked by the buildings, and typically nonline-of-sight (NLOS) multipath conditions predominate. The design of indoor positioning systems is challenging as the rich indoor multipath radio propagation environment makes accurate TOA measurements difficult. In particular, the scattering of the radio signals results in TOA measurement errors consisting of a biased component as well as a zero-mean random error typical of LOS outdoor positioning systems. In the presence of multipath signals, the classical iterative LS algorithm does not perform well, so that more complex and computationally intensive methods are required to mitigate the effects of multipath bias errors [5, Chapters 10 and 12]. These methods include improved TOA estimation such as leading edge detection algorithms [12], and complex position determination algorithms that attempt to detect large range errors and appropriately weight or eliminate these data in the position determination process [5]. An alternative, simpler approach is pursued in this paper, based on modeling the bias errors in an indoor environment.

While in an outdoor environment the multipath bias effect cannot be easily modeled due to the great variability in the operating conditions, NLOS indoor measurements show [5], [13], [14], [15], [16] that the TOA bias can be approximately modeled as a linear function of range. This effect is based on the quasi-homogeneous structure of many buildings and the consequential signal scattering, so that the zig-zag path from the transmitter to the receiver causes

- *I. Sharp is with the Wireless and Networking Technologies Laboratory, ICT Centre, CSIRO, Marsfield NSW 2122, Australia. E-mail: isharp25@optusnet.com.au.*
- *K. Yu is with the School of Surveying and Spatial Information Systems, University of New South Wales, Sydney, NSW 2052, Australia. E-mail: Kegen.Yu@ieee.org.*

Manuscript received 20 July 2011; revised 26 Mar. 2012; accepted 18 May 2012; published online 31 May 2012.
For information on obtaining reprints of this article, please send e-mail to: tmc@computer.org, and reference IEEECS Log Number TMC-2011-07-0402. Digital Object Identifier no. 10.1109/TMC.2012.124.

1536-1233/13/$31.00 © 2013 IEEE Published by the IEEE CS, CASS, ComSoc, IES, & SPS
Authorized licensed use limited to: DSTA. Downloaded on May 04,2020 at 12:45:52 UTC from IEEE Xplore. Restrictions apply.

an increase in the range excess with range, which to a first order is a linear function of range. Additionally, a range-independent delay is associated with the TOA detection of the scattered incident NLOS signals arriving at the receiver. Thus, the indoor bias errors can be modeled as a constant offset plus a linear range-bias component, namely

$$\Delta r_{bias} = \delta r_0 + \lambda r, \tag{1}$$

where λ is the range bias error parameter, and δr_0 is the ranging offset error which is common to all the measurement paths. Note that with this ranging error model, the δr_0 offset effect turns range measurements into pseudo-range measurements. If the two propagation parameters in (1) can be estimated, the effect of the ranging bias errors can be significantly reduced, and hence, the positional accuracy can be improved to close to the LOS case where only the zero-mean random errors occur. Indeed, it can be shown from [6] that the LS linearization method described in Section 2 can approach the best linear unbiased estimate (BLUE) provided the following conditions apply:

1. The random noise in the range measurements are uncorrelated and Gaussian.
2. The random errors STD is much smaller than the ranges.
3. Range-related bias errors are removed.

The measured data presented in Fig. 2 show that the first condition is approximately true, provided the condition 3 is applied. Condition 2 is approximately valid, except for locations near BSs. Further, the BLUE solution will approach the minimum geometric dilution of precision (GDOP) if the node geometry is symmetric relative to the location being determined, and hence also approaches the CRLB due to its equivalence with minimum GDOP [17], [18]. This geometrical condition approximately applies to a mesh network of BSs with approximately (statistical) uniform spatial distribution. Thus, in summary, provided the range bias errors are removed (the subject of the paper), the LS performance will be asymptotically close to the CRLB as the range STD to range ratio approaches zero.

The main contributions of this paper can be summarized as follows:

1. The development of an enhanced LS positioning algorithm that takes into account the bias errors associated with indoor range measurements. Both the range and pseudo-range cases are analyzed.
2. The derivation of general analytical expressions for the enhanced LS solution based on an existing known solution, such as the classical LS algorithm.
3. The derivation of expressions for the bias parameters which minimize the mean-square error of the position coordinate estimation. Accordingly, the enhanced LS algorithm approaches the optimal solution in terms of minimization of mean-square error.
4. The testing of the derived analytical expressions with simulated and experimental data. A real mesh network positioning system has been developed and its performance is examined through experiments. The positional accuracy of the classical and enhanced LS algorithms is compared using both range and pseudo-range measurements.

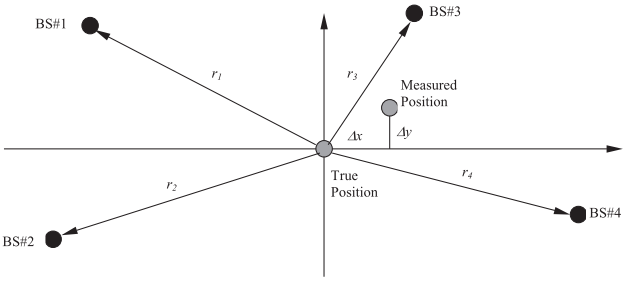

Fig. 1. Geometry of the mobile node in relationship to the fixed nodes.

The remainder of the paper is organized as follows: Section 2 briefly reviews the theory and concepts of both range and pseudo-range position determination using the enhanced LS positioning algorithm, and the consequential errors when the TOA measurements have both random and bias errors. Section 3 describes some of the characteristics of the enhanced LS algorithm, including its relationship to the standard LS algorithm and analytical expressions for the random and bias positional errors. Section 4 describes a method of determining the bias parameters $(\lambda, \delta r_0)$ from measured data in a mesh network, and the associated optimum λ_{opt}. Section 5 presents experimental results obtained by conducting measurements in a typical office building complex using a real TOA-based mesh-network positioning system, and compares the positional performance with the analytical expressions. Finally, Section 6 concludes the paper.

2 Enhanced Iterative LS Method

This section summarizes the theory of computing a position based on measured ranges or pseudo-ranges from fixed nodes in a mesh network. The analysis is essentially the classical theory of radio navigation, but with modifications to include the effects of ranging bias errors.

2.1 Position Determination Analysis

The following analysis summarizes the classical least-squares fit (LSF) approach for the determination of the position of a mobile node using range or pseudo-range measurements to a number of fixed nodes. The measurements will have errors associated with system noise and multipath propagation. The two-dimensional geometry of the problem is illustrated in Fig. 1. The true position of the mobile node is located at the origin of the x-y axes. Denoting the mobile and the ith BS position as (x, y) and (x_i, y_i), respectively, the ranges from the mobile to the BSs are

$$r_i = \sqrt{(x_i - x)^2 + (y_i - y)^2}, \quad i = 1, 2, \ldots, N_R, \tag{2}$$

where N_R BSs are within the radio range of the mobile unit. Depending on the type of system, the BSs will measure either range or pseudo-ranges. For range measurements, typical implementation (and in particular the measurements described in Section 5) is based on the round-trip time (RTT) between two nodes. Note in this particular case, the internal delays in the radios and the baseband circuitry needs to be subtracted from the RTT to obtain the propagation delay (and hence the range), so that accurate

Authorized licensed use limited to: DSTA. Downloaded on May 04,2020 at 12:45:52 UTC from IEEE Xplore. Restrictions apply.

Fig. 2. Measured ranging error performance based on RTT measurements between pairs of nodes scattered throughout the building complex shown in Fig. 4. The measured parameters are: $\lambda = 0.020$ and $\sigma_r = 0.94$ m. The solid line is the associated linear LSF model, and the dotted lines are $\pm\sigma_r$ relative to the linear trend line. The zero-range bias error is $\delta r_0 = 0.52$ m.

estimates of internal delays need to be determined in addition to the RTT. For pseudo-range measurements, if the clocks in the BSs are suitably synchronized, the relative transmit timing and the transmitter equipment delays will be common to all the measurements in the BS receivers, and thus form part of the pseudo-range offset constant. As a consequence, the delays in the receivers are not required to be determined for pseudo-range position determination. Because of these characteristics, pseudo-range measurements are often preferred over range measurements, particularly for more accurate positioning. Further, as will be shown, pseudo-ranges have other advantages for indoor positioning when there are measurement bias errors due to the radio propagation characteristics.

For this analysis, it is assumed that the indoor propagation results in both a positive bias which is proportional to the propagation range plus a nonzero offset, and a zero-mean random component which is independent of range. This assumed error model is supported (at least approximately) by indoor radio propagation measurements [13], [14], [15], [16], as well as the measurements described in Section 5. While measurements show a tendency for the random variation to increase with range, this increase is largely associated with a small fraction of the data that exhibit range errors greater than the time resolution (pulse rise-time) of the TOA measurement. For practical indoor positioning, these large "pathological" errors need to be detected and eliminated [5, Chapters 10, 12, and 19]. It will be shown in Section 5 that when these large errors are eliminated, the residual random errors have a variation which is largely independent of range. Based on these assumptions, the measured pseudo-range p_ε associated with the ith BS is given by

$$\begin{aligned} p_{\varepsilon_i} &= p_i + \varepsilon(0, \sigma_r), \\ p_i &= f(x, y, \phi; \lambda, \delta r_0) = r_i + c\phi + (\delta r_0 + \lambda r_i) \\ &= (1+\lambda) r_i + (c\phi + \delta r_0), \end{aligned} \tag{3}$$

where ε is the zero-mean random error with STD σ_r, c is the speed of propagation (0.3 meters per nanosecond), and ϕ is the timing phase of the clock in the mobile node relative to the time-synchronized BSs ($\phi = 0$ for range measurements). Note that in the case $\lambda = 0$, $\delta r_0 = 0$ and (3) becomes the classical formulation of the problem, and is typically applied to the indoor case even though it does not accurately describe the problem. In general, the values of λ and δr_0 in a given propagation environment will not be known, but it will be shown later in Section 4 how these parameters can be estimated. To illustrate these concepts, an example of the measured data from the positioning system described in Section 5 is shown in Fig. 2. Observe the linear trend in the bias, and also that the variation relative to the linear trend appears to be largely independent of range. Also, observe that this condition (constant STD) is a requirement for the LS algorithm to provide an optimum solution, as described in Section 1.

The nonlinear (3) needs to be solved for the position of the mobile node (x, y) . Because of the nonlinearity an analytical solution is difficult. One standard method [5], [20], [21], [22] in such cases is to linearize the equations to find an approximate solution, which can be iterated to obtain the final accurate numerical solution. In particular, (3) can be expanded as a first-order Taylor series, resulting in

$$p_{0_i} \approx f(x_0, y_0, b_0; \lambda) + \frac{\partial p_i}{\partial x}\Delta x + \frac{\partial p_i}{\partial y}\Delta y + \frac{\partial p_i}{\partial b}\Delta b, \tag{4}$$

where the initial (guess) starting point is at (x_0, y_0, b_0), typically chosen at the mean of the surrounding BS coordinates, and the combined bias term is $b = \delta r_0 + c\phi$. This first-order (linear) approximation improves as the range error to range ratio approaches zero. Note also that the bias term λ is assumed to be a parameter rather than a variable; the reason for this choice will be explained in Section 2.2.

Applying (4) with an estimate of the bias parameter defined as $\hat{\lambda}$ results in

$$\begin{aligned} \Delta\hat{p}_i &= \left(1+\hat{\lambda}\right)\left(\frac{x - x_i}{r_i}\right)\Delta x + \left(1+\hat{\lambda}\right)\left(\frac{y - y_i}{r_i}\right)\Delta y + \Delta b \\ &= (1+\hat{\lambda})\alpha_i \Delta x + (1+\hat{\lambda})\beta_i \Delta y + \Delta b, \end{aligned} \tag{5}$$

where $\Delta\hat{p}_i = p_{0i} - f(x_0, y_0, b_0; \hat{\lambda})$, $\alpha_i = \cos\theta_i = \frac{x - x_i}{r_i}$, and $\beta_i = \sin\theta_i = \frac{y - y_i}{r_i}$.

For the classical range case, it is assumed that $\Delta b = 0$. Note that (5) depends on the angular position θ_i of the mobile node relative to ith BS, and is independent of the associated range.

Equation (5) gives the measurements as a function of the positional and bias errors associated with the initial starting point for the iteration. However, the analysis requires estimates of the positional error in terms of the range errors. This is achieved by performing a LSF on the linear equations represented by (5), so that the differences between the measured pseudo-ranges/ranges and that given by (5) are minimized. It is convenient to perform the analysis using matrix algebra, so that (5) can be expressed as

$$\mathbf{A}\boldsymbol{\delta} = \boldsymbol{\Delta}\mathbf{p}, \tag{6a}$$

where, for pseudo-ranges,

Authorized licensed use limited to: DSTA. Downloaded on May 04,2020 at 12:45:52 UTC from IEEE Xplore. Restrictions apply.

$$\mathbf{A}=\begin{bmatrix}(1+\hat{\lambda})\alpha_1 & (1+\hat{\lambda})\beta_1 & 1\\ \vdots & \vdots & \vdots\\ (1+\hat{\lambda})\alpha_N & (1+\hat{\lambda})\beta_N & 1\end{bmatrix},\ \boldsymbol{\delta}=\begin{bmatrix}\Delta x\\ \Delta y\\ \Delta b\end{bmatrix},\ \boldsymbol{\Delta p}=\begin{bmatrix}\Delta\hat{p}_1\\ \vdots\\ \Delta\hat{p}_N\end{bmatrix} \tag{6b}$$

and, for ranges,

$$\mathbf{A}=\begin{bmatrix}(1+\hat{\lambda})\alpha_1 & (1+\hat{\lambda})\beta_1\\ \vdots & \vdots\\ (1+\hat{\lambda})\alpha_N & (1+\hat{\lambda})\beta_N\end{bmatrix},\ \boldsymbol{\delta}=\begin{bmatrix}\Delta x\\ \Delta y\end{bmatrix},\ \boldsymbol{\Delta p}=\begin{bmatrix}\Delta r_1\\ \vdots\\ \Delta r_N\end{bmatrix}. \tag{6c}$$

In typical practical situations, the linear (6) are overly defined (more than three BSs for pseudo-ranges and two BSs for ranges), so that a LS solution can be obtained from

$$\boldsymbol{\Phi}\delta=\mathbf{h}, \tag{7a}$$

where, for pseudo-ranges,

$$\boldsymbol{\Phi}=\mathbf{A}^{\mathrm{T}}\mathbf{A}=\begin{bmatrix}(1+\hat{\lambda})^2\sum_i\alpha_i^2 & (1+\hat{\lambda})^2\sum_i\alpha_i\beta_i & (1+\hat{\lambda})\sum_i\alpha_i\\ (1+\hat{\lambda})^2\sum_i\alpha_i\beta_i & (1+\hat{\lambda})^2\sum_i\beta_i^2 & (1+\hat{\lambda})\sum_i\beta_i\\ (1+\hat{\lambda})\sum_i\alpha_i & (1+\hat{\lambda})\sum_i\beta_i & N\end{bmatrix}$$

$$\mathbf{h}=\mathbf{A}^{\mathrm{T}}\boldsymbol{\Delta p}=\begin{bmatrix}(1+\hat{\lambda})\sum_i\alpha_i\Delta\hat{p}_i\\ (1+\hat{\lambda})\sum_i\beta_i\Delta\hat{p}_i\\ \sum_i\Delta\hat{p}_i\end{bmatrix} \tag{7b}$$

and, for ranges,

$$\boldsymbol{\Phi}=\begin{bmatrix}(1+\hat{\lambda})^2\sum_i\alpha_i^2 & (1+\hat{\lambda})^2\sum_i\alpha_i\beta_i\\ (1+\hat{\lambda})^2\sum_i\alpha_i\beta_i & (1+\hat{\lambda})^2\sum_i\beta_i^2\end{bmatrix},\quad \mathbf{h}=\begin{bmatrix}(1+\hat{\lambda})\sum_i\alpha_i\Delta r_i\\ (1+\hat{\lambda})\sum_i\beta_i\Delta r_i\end{bmatrix}. \tag{7c}$$

The solution to linear matrix equation (7a) can be expressed in the form

$$\boldsymbol{\delta}=\left(\mathbf{A}^{\mathrm{T}}\mathbf{A}\right)^{-1}\left(\mathbf{A}^{\mathrm{T}}\boldsymbol{\Delta p}\right)=\boldsymbol{\Phi}^{-1}\mathbf{h}. \tag{8}$$

The vector $\boldsymbol{\delta}$ provides an estimate for the correction required to the initial estimate of the three variables $\Delta x, \Delta y$, and Δb. Thus, better estimates for pseudo-ranges and ranges are

$$\begin{bmatrix}x_1\\ y_1\\ \phi_1\end{bmatrix}=\begin{bmatrix}x_0\\ y_0\\ \phi_0\end{bmatrix}+\begin{bmatrix}\Delta x\\ \Delta y\\ \Delta b\end{bmatrix}\text{or}\begin{bmatrix}x_1\\ y_1\end{bmatrix}=\begin{bmatrix}x_0\\ y_0\end{bmatrix}+\begin{bmatrix}\Delta x\\ \Delta y\end{bmatrix}, \tag{9}$$

where for the range case it is assumed that the constant bias error δr_0 has been independently estimated (see Section 4) and removed from the measured range data. If this procedure is not performed, then the nominal range data are actually pseudo-range data, and must be processed according to the pseudo-range method.

Equation (8) can be applied iteratively until the increments are sufficiently small. Note that these corrections are not the errors in the position of the mobile node, which are dependent on the measurement errors and the value of the parameter $\hat{\lambda}$, but are increments in the iterative process. As the solution converges, these increments will approach zero in most situations, although with large measurement errors the algorithm may not converge. Also note from a theoretical point of view, if the initial starting point is the true position, the first increment is an estimate of the position error of the LS algorithm, as the algorithm convergence essentially occurs with just one iteration. This procedure is essentially the calculation GDOP [18], [21], [22], after normalization by the range STD, and hence directly related to the theoretical limits defined in [17], [18], as discussed in Section 1.

2.2 Bias Parameter λ

The solution for the position of the mobile node as given by (8) and (9) will depend on the bias parameter $\hat{\lambda}$ chosen. The actual radio propagation parameter λ for the operating environment is typically not known, and thus, it appears that the LS solution should also estimate this parameter. However, the purpose of introducing the parameter λ to the LS solution is to improve the accuracy of the estimated mobile node positions when compared with the standard procedure where this parameter is not used ($\hat{\lambda}=0$). Thus, any change from the standard method should not result in a degrading in performance. The following summarize why it is not appropriate to include the parameter $\hat{\lambda}$ in the LS solution:

1. If the parameter $\hat{\lambda}$ is included as a variable, there will be a total of four[1] variables to be solved for, and hence at least four measurements at four BSs. In contrast, the standard solution only requires measurements from three BS to obtain a position fix. Thus, including the parameter $\hat{\lambda}$ will result in fewer positions being determined or less (or no) redundancy, resulting in less reliable positions.
2. The bias parameter λ is associated with the characteristics of the indoor radio propagation. By definition, this parameter can only be estimated by measurements at both short and long range, and thus, the $\hat{\lambda}$ parameter represents an average over a considerable area. An estimate based on one set of BS measurements will typically be over a much smaller area, and thus is a less reliable estimate compared with a more global estimate. In particular, averaging over many position estimates will be necessary for a good estimate of the parameter λ.
3. The classical approach of LS position determination effectively decouples the geometric factors (as expressed by the GDOP) and the propagation characteristics as expressed by the ranging error STD. Incorporating the parameter λ into the LS solution as a variable will couple these two components of the position accuracy.

1. While it may appear that for the range case, three base stations are required to solve the equations, this results in a two-way ambiguity in the computed position, so that in practice, at least four BSs are required.

Authorized licensed use limited to: DSTA. Downloaded on May 04,2020 at 12:45:52 UTC from IEEE Xplore. Restrictions apply.

4. If $\hat{\lambda}$ is a parameter rather than a variable, the parameter λ can be estimated by a separate process (as yet undefined) with appropriate smoothing and filtering, such as by applying a Kalman filter to the raw estimates from individual position fix data.
5. While the optimum solution may seem to occur when $\hat{\lambda} = \lambda$, it will be shown that in fact the optimum which minimizes the mean-square position errors is in fact a different, larger value. Thus, $\hat{\lambda} = \lambda_{opt}$ cannot be directly calculated by incorporating $\hat{\lambda}$ into the LS solution.

Thus, the algorithm defined in Section 2.1 assumes that $\hat{\lambda} = \lambda_{opt}$ is determined external to the position determination algorithm; details of this process are described in Section 4.

3 Enhanced LS Algorithm Characteristics

Section 2 described the proposed enhancements to the classical LS algorithm to account for bias errors. This section analyzes the characteristics of the enhanced algorithm.

3.1 Generalized Solution

As shown in Section 2.1, the performance of the enhanced LS algorithm can be determined by performing an analysis based on the general solution as defined by the matrix equation (8). However, suppose that a solution to the standard LS algorithm is known (either analytical or numerical), and from this solution, it is required to determine the enhanced LS solution without being involved with the details of the standard solution. In particular from (8), suppose the standard LS solution with $\hat{\lambda} = 0$ is given by

$$\boldsymbol{\delta}_0 = \boldsymbol{\Phi}_0^{-1}\mathbf{h}_0. \tag{10}$$

From (7) and (8), it can be observed that the $\boldsymbol{\Phi}$ matrix for an enhanced solution can be expressed as

$$\boldsymbol{\Phi} = \boldsymbol{\Lambda}\boldsymbol{\Phi}_0\boldsymbol{\Lambda} \text{ so that } \boldsymbol{\Phi}^{-1} = \boldsymbol{\Lambda}^{-1}\boldsymbol{\Phi}_0^{-1}\boldsymbol{\Lambda}^{-1}, \tag{11a}$$

where, for pseudo-ranges or ranges, respectively,

$$\boldsymbol{\Lambda} = \begin{bmatrix} (1+\hat{\lambda}) & 0 & 0 \\ 0 & (1+\hat{\lambda}) & 0 \\ 0 & 0 & 1 \end{bmatrix} \text{ or } \quad \boldsymbol{\Lambda} = \begin{bmatrix} (1+\hat{\lambda}) & 0 \\ 0 & (1+\hat{\lambda}) \end{bmatrix}. \tag{11b}$$

To calculate the enhanced solution $\mathbf{h}$ vector, it is convenient to consider the bias and random components of the error separately. Thus, considering the bias effect, the first element in the $\mathbf{h}$ vector is given by

$$\begin{aligned}(\mathbf{A}^{\mathrm{T}}\boldsymbol{\Delta}\mathbf{p})_1 &= (1+\hat{\lambda})\sum_i \alpha_i \Delta p_i = (1+\hat{\lambda})\sum_i \alpha_i(\lambda-\hat{\lambda})r_i \\ &= \left(\sum_i \alpha_i \lambda r_i\right)\left[\frac{(\lambda-\hat{\lambda})(1+\hat{\lambda})}{\lambda}\right].\end{aligned} \tag{12}$$

The last expression in (12) is the product of the standard LS algorithm bias component and a constant factor which is related to the actual and estimated propagation bias terms. The second component of the $\mathbf{h}$ vector is similar to the first, with β replacing α. The third component (pseudo-ranges only) can be similarly calculated as

$$\begin{aligned}(\mathbf{A}^{\mathrm{T}}\boldsymbol{\Delta}\mathbf{p})_3 &= \sum_i \Delta p_i = \sum_i (\lambda-\hat{\lambda})r_i \\ &= \left(\sum_i \lambda r_i\right)\left[\frac{\left(\lambda-\hat{\lambda}\right)}{\lambda}\right].\end{aligned} \tag{13}$$

Combining the components into a vector, the $\mathbf{h}$ vector related to the bias ($\mathbf{b}$) can be expressed in the form

$$\mathbf{h}^{\mathrm{b}} = \left[\frac{\lambda-\hat{\lambda}}{\lambda}\right]\boldsymbol{\Lambda}\mathbf{h}_0^{\mathrm{b}}. \tag{14}$$

Thus, the enhanced LS bias component of $\boldsymbol{\delta}$ is given by

$$\begin{aligned}\boldsymbol{\delta}^{\mathrm{b}} = \boldsymbol{\Phi}^{-1}\mathbf{h}^{\mathrm{b}} &= \left[\frac{\lambda-\hat{\lambda}}{\lambda}\right]\left(\boldsymbol{\Lambda}^{-1}\boldsymbol{\Phi}_0^{-1}\boldsymbol{\Lambda}^{-1}\right)\boldsymbol{\Lambda}\mathbf{h}_0^{\mathrm{b}} \\ &= \left[\frac{\lambda-\hat{\lambda}}{\lambda}\right]\boldsymbol{\Lambda}^{-1}\left(\boldsymbol{\Phi}_0^{-1}\mathbf{h}_0^{\mathrm{b}}\right) = \boldsymbol{\Omega}_{\mathrm{b}}\boldsymbol{\delta}_0^{\mathrm{b}},\end{aligned} \tag{15}$$

where $\boldsymbol{\Omega}_{\mathrm{b}} = [\frac{\lambda-\hat{\lambda}}{\lambda}]\boldsymbol{\Lambda}^{-1}$, $\mathbf{h}_0^{\mathrm{b}}$ is bias component of the $\mathbf{h}$ vector for the standard LS solution, and $\boldsymbol{\delta}_0^{\mathrm{b}}$ is bias component of the $\boldsymbol{\delta}$ vector for the standard LS solution.

Thus, if a solution is known for the standard LS algorithm, the corresponding enhanced LS solution can be derived by multiplication by the matrix

$$\boldsymbol{\Omega}_{\mathrm{b}} = \mathrm{diag}\left(\frac{\lambda-\hat{\lambda}}{\lambda(1+\hat{\lambda})} \quad \frac{\lambda-\hat{\lambda}}{\lambda(1+\hat{\lambda})} \quad \frac{\lambda-\hat{\lambda}}{1+\hat{\lambda}}\right)$$

or

$$\boldsymbol{\Omega}_{\mathrm{b}} = \mathrm{diag}\left(\frac{\lambda-\hat{\lambda}}{\lambda(1+\hat{\lambda})} \quad \frac{\lambda-\hat{\lambda}}{\lambda(1+\hat{\lambda})}\right) \tag{16}$$

for the pseudo-range and range cases, respectively. Now, consider calculating the random ($\mathbf{r}$) part of the $\mathbf{h}$ vector. The same procedure as described for the bias part results in the expression

$$\boldsymbol{\delta}^{\mathrm{r}} = \boldsymbol{\Phi}^{-1}\mathbf{h}^{\mathrm{r}} = \boldsymbol{\Lambda}^{-1}\boldsymbol{\delta}_0^{\mathrm{r}} = \boldsymbol{\Omega}_{\mathrm{r}}\boldsymbol{\delta}_0^{\mathrm{r}}, \tag{17}$$

where $\boldsymbol{\Omega}_{\mathrm{r}} = \boldsymbol{\Lambda}^{-1}$ and $\boldsymbol{\delta}_0^{\mathrm{r}}$ is random component of the $\boldsymbol{\delta}$ vector for the standard LS solution. Finally, adding the bias and random components, the total $\boldsymbol{\delta}$ vector is given by

$$\boldsymbol{\delta} = \boldsymbol{\Phi}^{-1}\mathbf{h} = \boldsymbol{\Omega}_{\mathrm{b}}\boldsymbol{\delta}_0^{\mathrm{b}} + \boldsymbol{\Omega}_{\mathrm{r}}\boldsymbol{\delta}_0^{\mathrm{r}}. \tag{18}$$

Thus, if the standard LS solution is known, the enhanced LS solution can be directly calculated using (18) without any detailed calculations. This procedure is particularly useful if analytical solutions using the standard method are known, as the enhanced analytical solutions can be obtained with minimal effort; this approach is used in the following section.

3.2 Biased Error Solution

Using the generalized theory for the enhanced LS algorithm given in Section 3.1, this section applies the theory by using the known classical LS algorithm to obtain the enhanced solution; this procedure greatly simplifies the analysis. The

Authorized licensed use limited to: DSTA. Downloaded on May 04,2020 at 12:45:52 UTC from IEEE Xplore. Restrictions apply.

distribution of BSs is assumed to have arbitrary geometry, although in practice it often can be approximated by a uniform random distribution (see the simulation in Section 4.1) surrounding the mobile node. The standard LS solution [22], [6, Chapter 9] can be expressed in terms of the mean and variance of the x-coordinate and y-coordinate position errors. An identical analysis applies to both the x-coordinate and y-coordinate errors, so only equations associated with the x-position errors are given in the following analysis.

The analysis in the references shows that for the bias-error case the x-position error is generally nonzero, and is given by

$$\left(\Delta x^b\right)_0 = \lambda \sum_{i=1}^{N_R} \Gamma_i r_i, \tag{19a}$$

where the subscript "0" indicates the standard LS algorithm solution, and for pseudo-range and range positioning, respectively

$$\begin{aligned} \Gamma_i &= \alpha_i \Phi_{1,1}^{-1} + \beta_i \Phi_{1,2}^{-1} + \Phi_{1,3}^{-1} \text{ or} \\ \Gamma_i &= \alpha_i \Phi_{1,1}^{-1} + \beta_i \Phi_{1,2}^{-1} \end{aligned} \tag{19b}$$

and N_R is the number of BSs in range of the mobile node; a similar expression can be derived for the y-position error, except that in this case

$$\begin{aligned} \Gamma_i &= \alpha_i \Phi_{2,1}^{-1} + \beta_i \Phi_{2,2}^{-1} + \Phi_{2,3}^{-1} \text{ or} \\ \Gamma_i &= \alpha_i \Phi_{2,1}^{-1} + \beta_i \Phi_{2,2}^{-1}, \end{aligned} \tag{19c}$$

respectively, for the pseudo-range and range cases. For the random case, the mean of the x-position error is zero, assuming the mean of the range errors is zero, and the random range errors are uncorrelated. The variance of the x-position error for the random case is given by

$$\left(\sigma_{\Delta x}^r\right)_0^2 = \sigma_r^2 \sum_{i=1}^{N_R} \Gamma_i^2. \tag{20}$$

The total error consists of bias and random components. The expected value of the square of the combined bias and random errors is given by

$$\left(\sigma_{\Delta x}\right)_0^2 = \left(\Delta x^b\right)_0^2 + \left(\sigma_{\Delta x}^r\right)_0^2. \tag{21}$$

From (18), it can be observed that the enhanced LS solution for x-position error involves only multiplication by a constant, so the x-position error for the bias case is given by

$$\Delta x^b = \frac{\lambda - \hat{\lambda}}{1 + \hat{\lambda}} \sum_{i=1}^{N_R} \Gamma_i r_i, \tag{22}$$

so that with $\lambda = \hat{\lambda}$, the x-position error will be zero using the enhanced LS algorithm. Similarly, the variance will be multiplied by the square of the constant. Thus, from (17), the variance in the x-position error for the enhanced LS associated with the random range errors is given by

$$\left(\sigma_{\Delta x}^r\right)^2 = \left(\frac{1}{1 + \hat{\lambda}}\right)^2 \sigma_r^2 \sum_{i=1}^{N_R} \Gamma_i^2. \tag{23}$$

The total x-position variance is the sum of these two components, similar to (21). For a given situation, the total x-position error will be a function of both the actual bias parameter (λ) and the algorithm estimate $(\hat{\lambda})$. Observe from (22) that if $\lambda = \hat{\lambda}$, the bias component is zero, but interestingly this is not the optimum value of the parameter $\hat{\lambda}$ for obtaining the smallest combined error in Δx. The determination of the optimum value and the consequential performance is considered in the next section.

4 Determination of the Bias Parameter

This section describes the analytical method of determining the optimum bias parameter, and how its can be calculated from measured data in a mesh positioning system.

4.1 Optimal Bias Parameter

The analysis in Section 3.2 showed that for the enhanced LS algorithm, there are two components of the computed position error, one associated with the random errors and one associated with the bias errors. These errors are a function of the actual range bias error parameter (λ), and also the estimate of this parameter $(\hat{\lambda})$. Again the analysis for the y-position error is identical to the x-position analysis, so only x-position error equations are included in the following analysis.

To obtain the optimum solution, it is suggested that expected value of the square of the x-position error should be minimized. Thus, from (22) and (23), the expression to be minimized is

$$\begin{aligned} \sigma_{\Delta x}^2 &= \left(\sigma_{\Delta x}^r\right)^2 + \left(\Delta x^b\right)^2 \\ &= \left(\frac{1}{1 + \hat{\lambda}}\right)^2 \left(\sigma_{\Delta x}^r\right)_0^2 + \left(\frac{\lambda - \hat{\lambda}}{1 + \hat{\lambda}}\right)^2 \left(\frac{\left(\Delta x^b\right)_0}{\lambda}\right)^2. \end{aligned} \tag{24}$$

The optimal position determination performance occurs when (24) is minimized by selecting the optimum value of $\hat{\lambda}$. By differentiating (24) with respect to $\hat{\lambda}$ and equating to zero, the optimum value can be calculated to be

$$\lambda_{opt} = \lambda + \frac{\rho^2}{1 + \lambda}, \tag{25}$$

where ρ is the dimensionless ratio given by

$$\rho = \frac{\left(\sigma_{\Delta x}^r\right)_0}{\left(\Delta x^b\right)_0 / \lambda} = \sigma_r \left(\sqrt{\sum_{i=1}^{N_R} \Gamma_i^2} \Big/ \sum_{i=1}^{N_R} \Gamma_i r_i \right). \tag{26}$$

Note that the term in brackets in (26) is solely a function of the geometry of the layout of the nodes in range of the mobile node. From (25), it can be observed that the optimum bias parameter to be used in the enhanced LS algorithm is greater than the actual bias parameter associated with the radio propagation. Using (26) in (25), the mean square of the x-coordinate of the position error for the enhanced LS solution can be calculated to be

$$\left[\left(\sigma_{\Delta x}^r\right)^2 + \left(\Delta x^b\right)^2\right]_{opt} = \left(\sigma_{\Delta x}\right)_{opt}^2 = \frac{\left(\sigma_{\Delta x}^r\right)_0^2}{\left(1 + \lambda\right)^2 + \rho^2}, \tag{27}$$

Authorized licensed use limited to: DSTA. Downloaded on May 04,2020 at 12:45:52 UTC from IEEE Xplore. Restrictions apply.

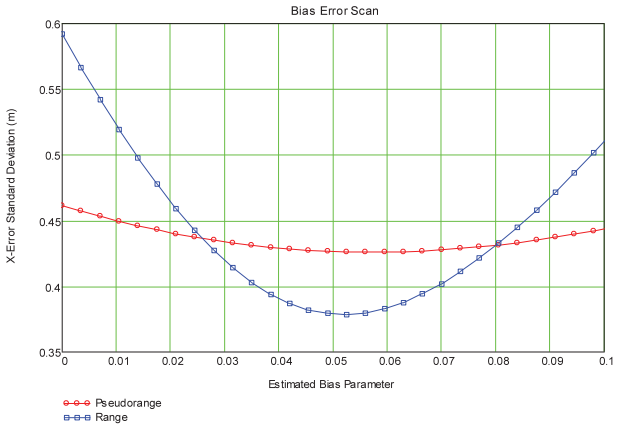

Fig. 3. Example of the simulated performance of the enhanced LS range algorithm for pseudo-range and range positioning. The parameters are: $\lambda = 0.035$, $\delta r_0 = 0.5$ m, $\sigma_r = 1$ m, $R_{\max} = 30$ m, and $N = 46$ BSs randomly located in a square area of $10{,}000\ \mathrm{m}^2$. The data are averaged over 1,000 simulated sets of BS locations.

which is less than the corresponding value based on the standard LS solution, namely

$$\sigma^2_{\Delta x} = \left(1 + \left(\frac{\lambda}{(1+\lambda)\rho}\right)^2\right)\left(\sigma^r_{\Delta x}\right)^2_0. \tag{28}$$

An example of the characteristics of the enhanced LS algorithm is shown in Fig. 3. The simulated data are for a coverage area of 10,000 square meters with 46 BSs (similar to the actual system described in Section 5). The results for measured data are given in Section 5. The BSs are located within the coverage area with a spatially uniform random distribution. Fig. 3 shows the variation in the STD of the x-coordinate error as a function of the algorithm estimated bias parameter $\hat{\lambda}$ for both pseudo-range and range positioning. As can be observed, using the standard LS algorithm $(\hat{\lambda} = 0)$, the pseudo-range positioning performance is much better than the corresponding range positioning performance, but at the optimum the range performance is superior; in general, pseudo-range positioning is less affected by bias errors. This result with bias errors is contrary to the classical solution with only random errors, where the range solution typically has superior accuracy compared with the pseudo-range solution.

The performance of a positioning system is often specified in terms of the mean radial error, as this measure can be readily determined from measured positional error data. The above analysis computes the STD in the x-coordinate (and y-coordinate) error only, but this measure can be converted into the equivalent mean radial error. Because the LS algorithm solution involves the summation of random components (see matrix equation (6)), the statistical distribution of the x- and y-coordinates will be approximately Gaussian due to the central limit theorem. Further, the x-coordinate and y-coordinate statistics are statistically independent, with approximately the same STD due to the approximately (statistical) uniform spatial distribution of the nodes in a mesh network. As a consequence, the radial distribution will have (approximately) Rayleigh statistics. For a Rayleigh distribution, the mean radial error is related to the 1D Gaussian distribution

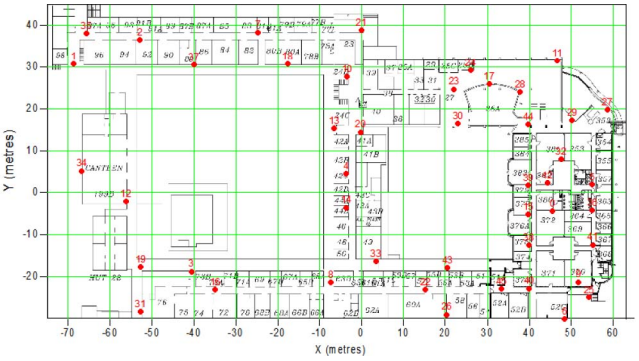

Fig. 4. Layout of site with buildings and the location of the 46 nodes. The area covered is around 10,000 square metres.

STD by the multiplication constant $\sqrt{\pi/2}$, so that equations such as (27) and (28) can be simply converted to the associated mean radial error.

4.2 Determining λ_{opt} from Measured Data

The application of the enhanced LS algorithm requires the determination of the optimum value of the bias parameter λ_{opt}. The optimum value is given by (25), which shows it is a function of two primary parameters, namely the environmental bias parameter (λ), the random range error STD (σ_r), as well as the geometry of the nodes. As the geometry is known, these two propagation related parameters need to be estimated from measurements (such as in Fig. 2) in the actual operating environment using the actual positioning system equipment, as the indoor propagating environment is usually too complex for mathematical modeling. Because the bias parameter requires measurements over a considerable area, the calculated parameters will be an overall average over the propagating environment, typically with one set of values for a whole building; for very large buildings dividing the total area into subregions may be appropriate. Assuming that the operating environment is static, the estimation of the parameters could be performed as part of the installation process, although real-time estimation would be more appropriate.

If the propagation parameters are determined as part of the installation process, then a basic survey of a building can be performed as follows: Two nodes of the positioning system are used to measure the RTT, and hence an estimation of the inter-nodal distances. The measurements require careful calibration of the radio equipment delays as well as accurate synchronization of the frequency in each node; time synchronization in the nodes is not necessary with the RTT technique [19], [23]. By accurately surveying the node positions by an independent method (usually using a plan of the building), a set of range errors versus range data can be obtained throughout the building. From this data set, the required parameters can be derived, as shown by the LSF lines in Fig. 2. An alternative to the above procedure is to survey the building using only the fixed BSs of the installed system, such as the nodes (BSs) shown in Fig. 4. A similar set of data to that described above can be obtained by measuring the range between every pair of BSs in the mesh network, resulting in a set of (at most) $N_{bs}(N_{bs}-1)/2$ range measurements. These measurements can be performed in real time as a "background" task

Authorized licensed use limited to: DSTA. Downloaded on May 04,2020 at 12:45:52 UTC from IEEE Xplore. Restrictions apply.

during the normal operation of the system, as calibration parameters such as equipment delays will vary over time [19], [23].

Having a set of N (calibrated) radio-measured and surveyed ranges $(\hat{R}_m, R_m)$ the bias parameter and the range error STD can be determined by a LS fitting process. In particular, defining the range error as $\Delta R_m = \hat{R}_m - R_m$, the estimated range bias parameters are given by

$$\begin{aligned}\lambda_{est} &= \frac{1}{\Delta}\left[N\sum_m R_m \Delta R_m - \sum_m R_m \sum_m \Delta R_m\right],\\ \delta r_0 &= \frac{1}{\Delta}\left[\sum_m \Delta R_m \sum_m R_m^2 - \sum_m R_m\left(\sum_m R_m \Delta R_m\right)\right],\end{aligned} \tag{29}$$

where $\Delta = N\sum_m R_m^2 - (\sum_m R_m)^2$. The random range error STD can then be calculated by

$$\begin{aligned}\varepsilon_m &= \Delta R_m - (\delta r_0 + \lambda_{est} R_m),\\ \sigma_r &= \sqrt{E[\varepsilon^2]}.\end{aligned} \tag{30}$$

Using the results from (29) and (30) in (25) and (26), an estimate of the optimal parameter λ_{opt} can be calculated, which in turn can be applied to the enhanced LS position determination procedure described in Section 2.1.

The estimated STDs in the bias parameters $(\delta r_0, \lambda_{est})$ and the random range error STD (σ_r) can be obtained from the regression analysis. For σ_r, the STD of its estimated value is about $\sigma_r/\sqrt{N}$, and for δr_0 about $\sigma_r\sqrt{3/N}$, where N is the number of measurements. The uncertainty in δr_0 thus adds statistically to the range error STD, resulting in σ_r increasing by the small factor of $\sqrt{1+3/N}$. As the number of such measurements is of the order of $N_{bs}^2/2$, for even moderately large mesh networks the number of measurements will be several hundred; thus, the uncertainty in determining σ_r will be $\sqrt{1/N + 3/N^2}$, or less than about 7 percent with $N > 200$ (6 percent for the wireless ad hoc system for positioning (WASP) data in Fig. 2). For λ_{est}, the estimate has a STD of about $3\sqrt{2}\sigma_r/\sqrt{N}R_{\max}$, which for the WASP data in Fig. 2 is 0.0042, or 21 percent of λ_{est}. The sensitivity of the solution to the value of the bias parameter (λ) is illustrated in Fig. 3. For pseudo-range positioning, the optimum solution is largely insensitive to the bias parameter, while for range positioning the effect on the bias error is considerably greater. However, even in the later case, due to the flat shape near the optimum, an accuracy of ± 20 percent appears to be adequate. As a consequence, uncertainty in determining bias parameter λ_{opt} will not greatly affect the improvement in the accuracy of the position determination using the enhanced LS algorithm.

5 Measured Performance

The theory presented in previous sections was tested with actual data from a real indoor positioning system. The layout of the buildings and the nodes is shown in Fig. 4. Note that all the nodes (BSs) in this example are indoors, as this paper is focused on position determination in an indoor environment. However, it is clear from the map of the building layout in Fig. 4 that some of the internodal radio paths are partially outdoors; these paths will be less affected by bias errors. The aim of using the experimental data is to confirm the above theoretical analysis, and to determine the improvement factors of the enhanced LS algorithm compared with the standard algorithm for both range and pseudo-range data.

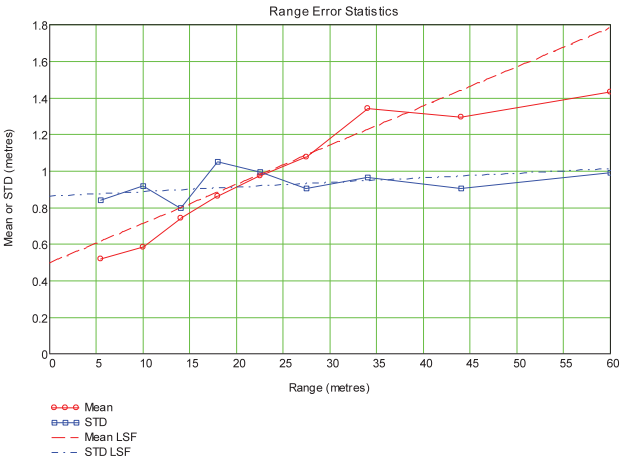

Fig. 5. Estimate of the mean and STD of the error data in Fig. 2 in "bins" of range. The bins size increases with range so that the number of samples (about 50) in each bin is approximately equal. The plotted points are at the centre of each range bin. The linear trendlines are based on a weighted (using the inverse of variance of the error) LSF.

The testing of the theoretical results was based on the WASP [12], [19], [23], developed by CSIRO. This experimental system operates in the 5.8-GHz ISM band with an effective bandwidth of 125 MHz. Position calculations are based on TOA estimation of a reconstructed wideband spread-spectrum signal with an effective leading-edge rise-time period of 13.5 nanoseconds; RTT between node pairs is determined from the TOA measurements. As part of the position determination process large range errors (approximately greater than the rise time) are eliminated [19] by a process of comparing the measured range with the range computed from the estimated position. Such a process is possible when there is redundancy in the number of BSs in range. The radio modules also support ad hoc data communications which allows the measured TOA data to be forwarded to a central data logging computer.

First, consider the determination of the bias and random parameters from measured data. Fig. 2 shows a scatter diagram of the measured range errors versus the range using intranodal RTT measurements. Observe that overall the range errors tend to increase with range, but the random component is approximately independent of range. A statistical analysis of the errors as a function of range is summarized in Fig. 5. The mean and STD of the error data were estimated in range "bins," so that the variation in these parameters can be estimated as a function of range. As can be observed the mean increases with range (approximately linearly), but the STD is approximately constant with range, as assumed in the theory. At long range, the mean errors are somewhat less than the linear trendline; the reason for this is that the long ranges include long obstacle-free paths outside the buildings (between the buildings—see Fig. 4), and thus the scattering effect will be less than for an all-indoor path. Note, however, all the nodes are within the buildings. Also note that there is a nonzero offset in the range errors at zero range, as was

Authorized licensed use limited to: DSTA. Downloaded on May 04,2020 at 12:45:52 UTC from IEEE Xplore. Restrictions apply.

assumed in the theory. This offset has no effect on the pseudo-range positioning performance, but does significantly affect the performance of range positioning.

From this data set, the theory in Section 3 can be used to obtain the estimated parameters: $\lambda = 0.020$ and $\sigma_r = 0.94$ m. Note in this case, the bias parameter λ is rather small, so the effects of ranging bias errors will not be very large. The low value of λ is in part due to the sophisticated leading edge algorithm [12] used to determine the TOA, but also the wide effective bandwidth of 125 MHz.

These results can be compared with some results reported in the literature. The simulations reported in [15] show that if data with errors greater than the rise time are eliminated, the range error scatter is approximately independent of range, supporting the WASP results. The measured UWB results in [16] show a similar characteristic regarding the range scatter, and an approximate linear bias as a function of range. However, the UWB measurements reported in [13], [14] are only presented in normalized form, the former normalized by $\log(1+r)$ and the latter by range. As raw (nonnormalized) data are not presented, the variation with range cannot be determined with any certainty. For example, in the latter case, 1 m error at 10 m range will have the same normalized error as a 10 m error at 100 m range. Further, as there are far more data at short range compared with long range, the normalized statistical distribution is dominated by the short-range data, so that the statistics of the raw data at long range cannot be inferred from the data in [14]. Further, as large range error data are not used for position determination, including such data are not appropriate for realistic performance estimates. Nevertheless, the normalized data [14] support the contention that the mean (bias) range errors increase with range, in agreement with the WASP data.

With the above data and the theory described in previous sections, the optimum bias parameter for the enhanced LS algorithm can now be determined. The data in Table 1 summarize the theoretical positioning performance based on the above theory and the measured range error STD, the range bias parameter, and the number of nodes in range. Both the pseudo-range and range positioning performance parameters are listed, as well as the parameters summarizing the node spatial distribution and the ranging performance, common to both. The random and bias position error parameters listed in Table 1 are defined as following:

$$\begin{aligned}(\sigma^r)_0 &= \sqrt{(\sigma^r_{\Delta x})_0^2+(\sigma^r_{\Delta y})_0^2},\\ (\Delta^b)_0 &= \sqrt{(\Delta x^b)_0^2+(\Delta y^b)_0^2},\\ (\sigma)_0 &= \sqrt{(\sigma^r)_0^2+(\Delta^b)_0^2},\end{aligned} \tag{31}$$

which are invariant to rotation.

From the data given in Table 1, the following observations can be made:

1. For the standard LS algorithm, the range positioning algorithm has superior performance with random errors (in line with theoretical expectations), but the pseudo-range positioning algorithm is superior with bias errors (in line with the above analysis).

TABLE 1
Summary of the Theoretical and Measured Parameters for the Indoor Test Case

Parameter	Pseudo-range	Range	Comment
σ_r	0.94 m	0.94 m	Random range error STD.
λ	0.020	0.020	Range error bias parameter.
$R_{\max}$	55 m	55 m	Average maximum radio range.
$\tilde{r}$	33 m	33 m	Average RMS radio range.
N_R	11	11	Typical number of nodes in radio range.
$(\sigma^r)_0$	0.72 m	0.60 m	Random errors - standard LS algorithm.
$(\Delta^b)_0$	0.36 m	0.69 m	Bias errors - standard LS algorithm.
ρ	0.0409	0.0178	Random STD to Bias STD ratio.
λ_{opt}	0.0220	0.0206	For enhanced LS algorithm.
$(\sigma)_0$	0.80 m	0.92 m	Overall STD - standard LS algorithm.
σ_{opt}	0.71 m	0.59 m	Overall STD - enhanced LS algorithm.
	11 %	36 %	Improvement factor.

2. Overall, pseudo-range positioning is superior when using the standard LS algorithm, while range positioning is superior when using the enhanced LS algorithm. Note, however, that this superior performance of the range-based positioning comes at the cost of the estimation and then the elimination of the constant range error δr_0.
3. The performance gain using the pseudo-range-based enhanced LS algorithm is rather modest (11 percent), while the performance gain using the range-based-enhanced LS algorithm is significant (36 percent).

The pseudo-range and range positioning performance as a function of the estimated linear bias parameter is shown in Fig. 6. As can be observed, without any correction (standard LS method), the pseudo-range performance is superior to the range performance, which is in agreement with the results in Table 1; using the enhanced LS algorithm with optimal estimation of the bias parameter $\hat{\lambda} = \lambda_{opt}$, the reverse is true, again in agreement with Table 1. Also shown in Fig. 6 for the range case is the effect of removing the offset bias (δr_0) from the measured data.

With the standard LS algorithm, the effect of removing the bias offset is significant but not optimum; the optimum using the enhanced algorithm is similar whether the offset bias is removed or not, although the optimum linear bias parameter $(\hat{\lambda})$ is different. However, it is also important to note that in actual situations, the measurement errors are not known, so that the performance scan shown in Fig. 6 cannot be used to find the minimum errors; the actual method of determining an estimate of the optimal value is by applying the method described in Section 3; these estimates are shown in Fig. 6, and can be observed to be close to the true optimum (curve minimum) for both ranges and pseudo-ranges.

Authorized licensed use limited to: DSTA. Downloaded on May 04,2020 at 12:45:52 UTC from IEEE Xplore. Restrictions apply.

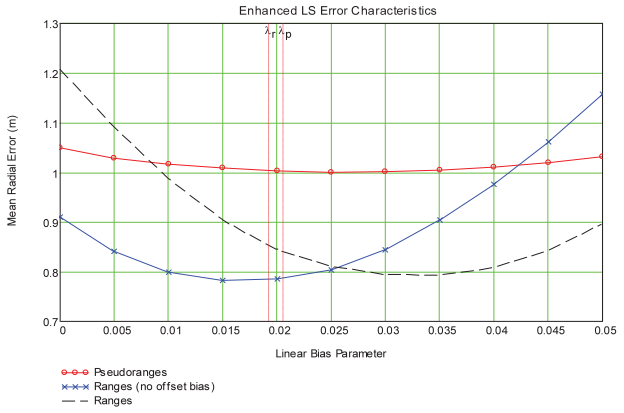

Fig. 6. Comparison of the performance of the enhanced pseudo-range and range LS positioning algorithm using the measured data. For the range case, the effect of removing the bias offset is also shown.

The overall statistical cumulative distribution function (CDF) of the positional errors is shown in Fig. 7a (pseudo-ranges) and Fig. 7b (ranges). From Fig. 7a, it can be observed that for pseudo-ranges, there is little difference between the standard and enhanced algorithms. In contrast, from Fig. 7b, it can be observed that the performance of the enhanced LS algorithm is considerably better than the corresponding standard algorithm. Thus, for example, if the "accuracy" of the positioning system is defined at a CDF of 0.7, the standard LS algorithm has errors of 1.0 and 1.6 m for, respectively, pseudo-range and range positioning; the corresponding values for the enhanced LS algorithm are 1.1 and 0.8 m. If the median (CDF $= 0.5$) is used as a reference, the standard and the enhanced range positioning errors are 1.3 and 0.65 m, respectively, resulting in accuracy improvement by a factor of 2.

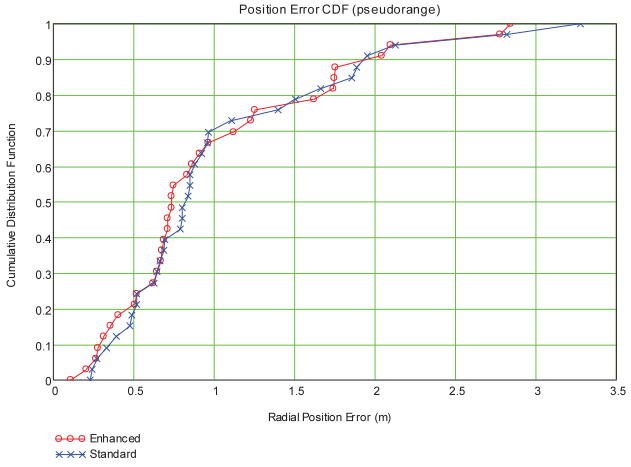

(a)

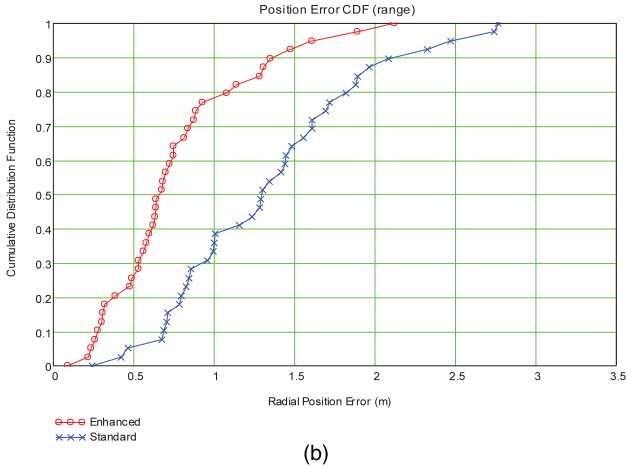

(b)

Fig. 7. (a) Comparison of the measured positional error CDFs using pseudo-ranges with the standard and enhanced LS positioning algorithms. (b) Comparison of the measured positional error CDFs using ranges with the standard and enhanced LS positioning algorithms.

6 Conclusions

This paper investigated the performance of an enhanced iterative LS positioning algorithm using both range and pseudo-range data in an indoor environment where the ranging errors include both a zero-mean random component and a range-dependent bias component. By modeling these latter bias errors as a linear function of range, an enhanced LS algorithm was developed to reduce the effects of the bias errors on the positional estimation. It is shown through analysis that in general, the enhanced LS algorithm can be related to the standard LS solution by simple scaling factors associated with the true range bias parameter and an estimate of the bias parameter. Further analysis shows that an optimum solution can be obtained from measurable data in a mesh network. Applying the theory to both pseudo-range and range data shows that the pseudo-range positioning with range bias errors is superior when using the standard LS algorithm, but that the range-based positioning is superior when using the enhanced algorithm. These theoretical results were confirmed with the results of processing range data from an actual mesh positioning system. As the enhanced LS algorithm can be easily applied for determining positions with essentially no extra data processing requirements over the standard LS method, it is suggested that the described enhanced method should be preferred for indoor positioning systems where a simple low-complexity algorithm is necessary, such as in wireless sensor network positioning.

Acknowledgments

The authors acknowledge the contribution of members of the Wireless Technologies Laboratory of the ICT Centre at CSIRO, including developing the WASP hardware and software, and assistance in performing the indoor experiments used in the analysis in this paper.

References

[1] J.A. Pierce, A.A. McKenzie, and R.H. Woodward, *Loran*, MIT Radiation Laboratory Series, vol. 4. McGraw-Hill, 1948.
[2] A. El-Rabbany, *Introduction to GPS: The Global Positioning System.* Artech House, 2002.
[3] P.J.G. Teunissen and A. Kleusberg, *GPS for Geodesy.* Springer, 1998.
[4] Q. Yihong and K. Hisashi, "On Relation among Time Delay and Signal Strength Based Geolocation Methods," *IEEE GlobeCom*, vol. 7, pp. 4079-4083, 2003.
[5] K. Yu, I. Sharp, and Y.J. Guo, *Ground-Based Wireless Positioning.* Wiley, June 2009.
[6] P.J.G. Teunissen, *Adjustment Theory: An Introduction.* VSSD, 2003.

Authorized licensed use limited to: DSTA. Downloaded on May 04,2020 at 12:45:52 UTC from IEEE Xplore. Restrictions apply.

[7] P. Bahl and V. Padmanabhan, "RADAR: An In-Building RF-Based User Location and Tracking System," *Proc. IEEE INFOCOM,* pp. 775-784, 2000.
[8] R.J. Fontana, E. Richley, and J. Barney, "Commercialization of an Ultra Wideband Precision Asset Location System," *Proc. IEEE Conf. UWB Systems and Technologies,* pp. 369-373, 2003.
[9] R.J. Fontana, "Recent System Applications of Short-Pulse Ultra-Wideband (UWB) Technology," *IEEE Trans. Microwave Theory and Technology,* vol. 52, no. 9, pp. 2087-2104, Sept. 2004.
[10] G. Chandrasekaran, M.A. Ergin, M. Gruteser, R.P. Martin, J. Yang, and Y. Chen, "DECODE: Exploiting Shadow Fading to Detect Comoving Wireless Devices," *IEEE Trans. Mobile Computing,* vol. 8, no. 12, pp. 1663-1675, Dec. 2009.
[11] C. Zhang, M.J. Kuhn, B.C. Merkl, A.E. Fathy, and M.R. Mahamed, "Real-Time Noncoherent UWB Positioning Radar with Millimetre Range Accuracy: Theory and Experiments," *IEEE Trans. Microwave Theory and Techniques,* vol. 58, no. 1, pp. 9-20, Jan. 2010.
[12] D. Humphrey and M. Hedley, "Super-Resolution Time of Arrival for Indoor Localization," *Proc. Int'l Conf. Comm.,* pp. 3286-3290, May 2008.
[13] B. Alavi and K. Pahlavan, "Modeling of the TOA-Based Distance Measurements Error Using UWB Indoor Radio Measurements," *IEEE Comm. Letters,* vol. 10, no. 4, pp. 275-277, Apr. 2006.
[14] N. Alsindi, B. Alavi, and K. Pahlavan, "Measurement and Modelling of Ultra Wideband TOA-Based Ranging in Indoor Multipath Environments," *IEEE Trans. Vehicular Technology,* vol. 58, no. 3, pp. 1046-1058, Mar. 2009.
[15] Alavi and K. Pahlavan, "Modeling of the Distance Error for Indoor Geolocation," *Proc. IEEE Wireless Comm. and Networking,* pp. 668-672, Mar. 2003.
[16] C. Gentile and A. Kik, "An Evaluation of Ultra Wideband Technology for Indoor Ranging," *Proc. IEEE GlobeCom,* pp. 1-6, 2006.
[17] J. Chaffee and J. Abel, "GDOP and the Cramer-Rao Bound," *Proc. Position Location and Navigation Symp.,* pp. 663-668, Apr. 1994.
[18] N. Levanon, "Lowest GDOP in 2-D Scenarios," *IEE Proc. Radar Sonar Navigation,* vol 147, no. 3, June 2000.
[19] T. Sathyan, D. Humphrey, and M. Hedley, "WASP: A System and Algorithms for Accurate Radio Localization Using Low-Cost Hardware," *IEEE Trans. Soc., Man and Cybernetics—Part C,* vol. 41, no. 2, pp. 211-222, Mar. 2011.
[20] Sokolnikoff and Redheffer, *Mathematics of Physics and Modern Engineering,* chapter 10, section 11. McGraw-Hill, 1966.
[21] I. Sharp, K. Yu, and M. Hedley, "On the GDOP and Accuracy for Indoor Positioning," *IEEE Trans. Aerospace and Electronic Systems,* vol. 48, no. 3, pp. 2032-2051, July 2012.
[22] I. Sharp, K. Yu, and Y.J. Guo, "GDOP Analysis for Positioning System Design," *IEEE Trans. Vehicular Technology,* vol. 58, no. 7, pp. 3371-3382, Mar. 2009.
[23] M. Hedley, D. Humphrey, and P. Ho, "System and Algorithms for Accurate Indoor Tracking Using Low-Cost Hardware," *Proc. IEEE/IOA Position, Location and Navigation Symp.,* pp. 633-640, May 2008.

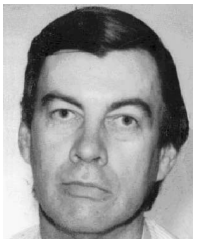

Ian Sharp is a senior consultant on wireless positioning systems. He has more than 30 years of engineering experience in radio systems. His initial involvement in positioning technology was in aviation, and later in the 1980s with the Interscan microwave landing system. In the later 1980s to the early 1990s, he was the research and development manager for the Quiktrak covert vehicle tracking system. This system is now commercially operating worldwide. From the mid-1990s to 2007, he worked at CSIRO mainly on developing experimental radio systems. He was the inventor and architect designer of CSIRO's precision location system (PLS) for sports applications. The PLS has been successfully trialed in Australia and the US. He holds a number of patents relating to positioning technology. He is a coauthor of the book: *Ground-Based Wireless Positioning* (Wiley and IEEE Press, 2009).

Kegen Yu received the PhD degree in electrical engineering from the University of Sydney in 2003. He initially worked as an associate engineer at Jiangxi Geological and Mineral Bureau, and then was an associate lecturer and, later, lecturer in the Department of Industrial Automation at Nanchang University. Subsequently, he was postdoctoral research fellow at the Centre for Wireless Communications, University of Oulu; a research scientist at the CSIRO ICT Centre; and a research fellow in the Department of Electronic Engineering at Macquarie University. Currently, he is a senior research fellow at the Australian Centre for Space Engineering Research and the School of Surveying & Geospatial Engineering, University of New South Wales, and an adjunct professor at Macquarie University. He is currently on the editorial boards of the *EURASIP Journal on Advances in Signal Processing*, *IEEE Transactions on Aerospace and Electronic Systems*, and *IEEE Transactions on Vehicular Technology*. He is the lead guest editor for a special issue of *Physical Communication* on "indoor navigation and tracking" and for a special issue of the *EURASIP Journal on Advances in Signal Processing* on "GNSS remote sensing." He coauthored the book *Ground-Based Wireless Positioning* (Wiley and IEEE Press; a Chinese version of the book is also available) and book chapters in three other books published by Wiley. He has also authored or coauthored about 30 refereed journal papers and more than 30 refereed conference papers. His current research interests include ground-based and GNSS-based positioning and GNSS remote sensing. He is a senior member of the IEEE.

▷ **For more information on this or any other computing topic, please visit our Digital Library at** www.computer.org/publications/dlib.

Authorized licensed use limited to: DSTA. Downloaded on May 04,2020 at 12:45:52 UTC from IEEE Xplore. Restrictions apply.